Radiation Physics and Chemistry 198 (2022) 110200

Contents lists available at ScienceDirect

Radiation Physics and Chemistry

journal homepage: www.elsevier.com/locate/radphyschem

Characterization of a thin photodiode as a routine dosimeter for low-dose radiation processing applications

Josemary A.C. Gonçalves [a], Alessio Mangiarotti [b], Carmen C. Bueno [a,*]

[a] Instituto de Pesquisas Energéticas e Nucleares, 05508-000, Cidade Universitária, São Paulo, Brazil
[b] Instituto de Física - Universidade de São Paulo, 05508-080, Cidade Universitária, São Paulo, Brazil

ARTICLE INFO

Keywords:
Radiation processing dosimetry
Si PIN Diode dosimeter
Gamma dosimetry

ABSTRACT

The characterization of a dosimetry system based on a commercial PIN photodiode as a routine dosimeter in a ^{60}Co industrial facility is reported. The main parameters of the dose rate response (repeatability, reproducibility, and angular dependence) and the dose response (dependence on both dose rate and accumulated dose) are investigated. The results obtained, within a dose rate range of 3.7–52.8 Gy/h and doses up to 200 Gy, fully adhere to the standard protocols established for radiation processing dosimetry. The diode performance as a routine dosimeter is validated by the good overall agreement with radiochromic films and alanine dosimetry.

1. Introduction

The trend toward low-dose radiation processing applications (Shastry et al., 2013; Salem et al., 2014; EL-Degwi and Gabarty, 2015; ISO/ASTM 51939, 2017) has increased interest in dosimetry systems with operational dose ranges extending to a few dozen Gy. Alanine and radiochromic films, among the dosimeters available for radiation processing dosimetry, are the ones suitable for measuring less than 100 Gy. Alanine is a reference standard dosimeter and, due to the advent of less expensive electron spin resonance spectrometers with user-friendly readout, has also been used as a routine dosimeter (ISO/ASTM 51607, 2013). Radiochromic films, whose dosimetric parameter is the color change after irradiation, also play an important role in routine radiation processing dosimetry (ISO/ASTM 51275, 2013).

However, the dosimetry optimization of the low-dose irradiation processes requires complementary dosimeters with prompt readout, easy handling, and cost-effectiveness. These features are found in active dosimeters based on ionization chambers and semiconductor devices such as transistors and diodes (Oliveira et al., 2000; Fuochi et al., 2004; Sephton et al., 2007; Bailey et al., 2009; Andjelković Ristić, 2013; 2015; Majer et al., 2019; Bueno et al., 2022). Regarding ionization chambers, attention must be paid to the design and insulating materials chosen for their construction due to the potential for radiation damage effects. Dosimeters based on metal-oxide-semiconductor field-effect transistors (MOSFET) have been designed for measuring absorbed doses using the shift in the threshold voltage caused by the trapped charge in the multilayered zones. However, an ordinary MOSFET is prone to radiation damage precluding its use for doses higher than a few hundred Gy (ICRU Report 80, 2008). Silicon diodes are also poorly resistant to radiation, but their simpler structures minimize the damaging effect on their dosimetric performance compared to transistors.

Pioneering feasibility studies on diodes for radiation processing dosimetry are available in the literature (Muller, 1970a, b; Osvay et al., 1975; Möhlmann, 1981; Dixon and Ekstrand, 1982). The operational principle of these dosimeters relies on the real-time acquisition of the induced currents from the irradiated diode operating in the short-circuit mode without externally applied voltage. Under this condition, the authors reported linear dose and dose rate responses, high current sensitivity, and good spatial resolution of such dosimeters. However, they highlighted two shortcomings: i) the gradual and continuous decay of the sensitivity with increasing accumulated dose; ii) the poor reproducibility of the electrical characteristics of the diodes even for those of the same type and batch. The former shortens the diode lifespan making periodic sensitivity checks necessary, while the latter gives rise to significant dosimeter-to-dosimeter response variability requiring a sample-specific dosimetric calibration. These drawbacks explain why silicon diodes are not recommended for radiation processing dosimetry (ICRU Report 80, 2008; ISO/ASTM 51649, 2015).

However, this scenario has been changed by the constantly improving industrial production of semiconductor devices and a better knowledge of the physical phenomena underlying the drop in the diode sensitivity with increasing doses. In high-energy physics experiments,

* Corresponding author. Cidade Universitária, Av. Lineu Prestes 2242, 05508-000, São Paulo, SP, Brazil.
E-mail address: ccbueno@ipen.br (C.C. Bueno).

https://doi.org/10.1016/j.radphyschem.2022.110200
Received 27 October 2021; Received in revised form 25 April 2022; Accepted 27 April 2022
Available online 9 May 2022
0969-806X/© 2022 Published by Elsevier Ltd.

much of this knowledge stems from developing silicon diodes more resistant to radiation damage induced by photons, neutrons, and ionized particles (Moll, 2018). For an unbiased diode, the current sensitivity decay is closely related to the decrease in the minority carrier diffusion length and, consequently, the reduction in the sensitive volume (Osvay and Tárczy, 1975; Casati et al., 2005; Bruzzi et al., 2007). One approach to keep this volume almost constant is to use thin diodes, i.e., with thicknesses smaller than the minority carrier diffusion length expected at the foreseen maximum accumulated dose. Commercial thin photodiodes (SFH206K) have been investigated for gamma and electron beam processing dosimetry, focusing on their sensitivity variation with the accumulated doses up to a few dozen kGy (Gonçalves et al., 2020, 2021). The results of the sensitivity decay (5% at 15 kGy) were found to be much smaller than those reported in the literature (Osvay and Tárczy, 1975; Grusell and Rikner, 1984; Gilar and Petr, 1985; Rikner Grussel, 1987; Barthe, 2001). In line with these previous findings, this work aims to provide a performance characterization of these diodes to check whether they can be used as routine dosimeters for low-dose radiation processing applications.

2. Materials and methods

2.1. Dosimetry probe and irradiation facility

Fifteen samples of the PIN silicon photodiode SFH206K, manufactured by Osram, with a full wafer thickness of (230 ± 5) μm and a square-shaped sensitive area of 7.02 mm^2 into a 5 mm plastic package, were used in this work. Dynamic measurements of the dark current versus reverse voltage (I–V curves) were performed using a semiconductor device analyzer (Keithley, model 2450) to assess the batch uniformity. At room temperature (22 °C), all devices exhibited low dark currents with less than 3% variations. Moreover, I–V curves were also measured at different room temperatures (18–26 °C) to determine the sensitivity variation with temperature (SVWT) of these diodes. The result obtained (0.3%/°C at 10 V) agreed, within the experimental error, with the one (0.2%/°C at 10 V) provided by the manufacturer.

Each diode was housed in a light-tight dosimetric probe, consisting of a polymethylmethacrylate (PMMA) cylinder (7 mm in diameter with 1 mm thick walls) coupled to a miniature coaxial connector (Lemo®). The electrical connection between the readout p-layer electrode and a Keithley 6517B electrometer was made via the inner conductor of a 20 m long coaxial cable, the circuit being closed by the woven shield. Current measurements were performed without externally applied voltage to the diode and its backplane grounded. The data acquired by the electrometer were directly sent to a personal computer via a GPIB interface to analyze the current signals. In addition, room temperature fluctuations (22 ± 2) °C were continuously monitored through a thermopar type K placed close to the probe. Under this condition, the sensitivity variation with the temperature of the unbiased diode was neglected and the current data were not corrected for.

The irradiations were performed with gamma rays from a ^{60}Co Panoramic irradiator (FIS 60–04, Yoshizawa Kiko Ltd), which contains one radioactive source in the form of a single pencil. Under irradiation conditions, the source is raised from a lead-shielded storage area and mechanically positioned at the center of a stainless steel base plate engraved with six circles (radii 16–66 cm) concentric with the radioactive source configuration. This geometry allows diodes and other dosimeters to be irradiated at different positions, hence different dose rates, at precise distances from the ^{60}Co source. Dose-rate calibrations were previously accomplished through standard reference alanine dosimeters with an expanded uncertainty of 1.7% (k = 2), traceable to the secondary standard laboratory at the International Atomic Energy Agency (IAEA).

2.2. Dose rate response

The dose-rate response was investigated by measuring the induced current as a dose rate function between 3.7 Gy/h and 52.8 Gy/h. Variation of the dose rate was accomplished by changing the diode-source distances from 66 to 16 cm. The diode was irradiated at each position during 300 s, and the corresponding induced current was continuously acquired by the electrometer operating in the high accuracy mode (0.5 s acquisition time). After each step of irradiation, with the source shielded, the background current was measured during 120 s to provide the signal-to-noise ratio and monitor the onset of radiation damage effects.

2.2.1. Repeatability

The repeatability parameter was assessed by the coefficient of variation CV (percentual ratio of the standard deviation to the average value) of five current signals delivered by the diode under consecutive irradiation cycles by switching on and off the ^{60}Co facility system. Measurements were performed at 3.7 Gy/h and 52.8 Gy/h dose rates.

Each induced current signal was acquired at a constant dose rate for 300 s, followed by a pause of 120 s. Thus, during the irradiation cycles, the currents (signal and background) were continuously recorded.

2.2.2. Reproducibility

The response reproducibility was measured monthly, irradiating the diode over one semester under reference conditions regarding positioning, exposure time, and dose rates from 3.7 to 52.8 kGy/h. Throughout the measurements, dose rates were corrected for the source activity decay. In between each set of measurements, all diodes were kept in a non-vacuum glass desiccator to protect them from moisture and temperature variations.

2.2.3. Angular response

The angular response, i.e., the change in the current sensitivity with the radiation incidence angle, was investigated by rotating the diode from 0° to 90° at intervals of 10°. The currents delivered by the diode settled at each position were registered during 300 s at a constant dose rate (52.8 Gy/h). All current data were normalized to unity at an incident angle of 0°. Zero degrees corresponds to the normal incidence of the gamma rays onto the front surface of the diode.

2.3. Dose response

The dose response was gathered offline by integrating the current signals, which gives the charge produced in the diode sensitive volume, as a function of the absorbed dose. The results attained at the same dose rate (52.8 Gy/h) were analyzed concerning linearity and charge sensitivity responses covering doses up to 200 Gy. The charge sensitivity is given by the slope of the charge versus the absorbed dose plot.

The effect of the accumulated dose on the dose response was indirectly assessed through the charge sensitivity parameter of a pristine diode and after being irradiated to 15 kGy, fractionated in three steps of 5 kGy. These irradiations were performed in a ^{60}Co Gammacell-220 irradiator type I (Atomic Energy of Canada Limited) under a dose rate of 628 Gy/h to reduce the exposure time.

The dose response dependence on the dose rate was investigated by irradiating the diode at different dose rates (3.7–52.8 Gy/h) to a constant dose of 7 Gy. The variation in the charge delivered by the diode was used as a parameter to infer the dose rate effect on the dose response.

2.4. Diode response as a routine dosimeter

In-plant irradiations of the diode and reference standard alanine dosimeters were performed to cover doses up to 200 Gy under a constant dose rate (52.8 Gy/h). Three alanine pellets of 93% alanine and 7% binder (Aerial, France) with 4.0 mm in diameter and 2.2 mm in height

were irradiated for each dose. The spectrum acquisition was performed with an MS400 ESR spectrometer (Magnettech, Berlin) equipped with the AerEDE dosimetry software (Aerial, France). The measurement parameters were set up as follows: microwave power of 8 mW, magnetic field centered at 3370 G with field sweep of 30 G, ten 12 s scans, a gain of 10^2, and 180° phase. The readouts were converted to dose through an alanine calibration curve earlier attained under the same conditions of use, specific to the irradiator, spectrometer, and dosimeter type (ISO/-ASTM 51607, 2013). A set of alanine pellets were irradiated at 52.8 Gy/h under exposure times settled to achieve doses between 5 and 200 Gy. Before and after each run of measurements, a reference dosimeter was read to ensure the spectrometer's stability. Four pellets (Aerial) were used for each step of irradiation, and the corresponding average readings were plotted as a function of the dose. The point values, distributed in a geometric sequence to cover 200 Gy, were best fitted by a linear function. The standard deviation of the points from the fit was 2.2%.

For comparative purposes, another well-established routine dosimeter, a radiochromic dye film, namely GAFChromic HD-V2, was also irradiated with alanine at the same position and dose values assessed with the diode. The film is comprised of a 12 μm thick active layer containing the marker dye and stabilizers, coated on a clear 97 μm polyester substrate usually supplied in a sheet of 8″ × 10″ size. The active coating reacts to form a uniform deep-blue colored polymer with maximum absorption at almost 670 nm upon irradiation. So, the radiation-induced increase in absorbance was measured with a Genesis-20 spectrophotometer (Thermo Scientific) at a peak absorbance wavelength of 670 nm. Before and during the irradiation, each dosimeter, a 0.3″ × 1.8″ strip dimensioned to fit the film holder of the spectrophotometer, was kept in a sachet to seal it against light and relative humidity effects. The absorbance readings were converted to dose with a GAFChromic HD-V2 and spectrophotometer-specific calibration curve assessed under procedures appropriate to comply with ISO protocols. Irradiations were performed at 52.8 Gy/h to doses ranging from 5 to 200 Gy in geometrical progression steps. Four films dosimeters were used for each dose, and the respective average absorbance values were plotted as a function of the dose. The best fitting of the data was achieved with a fourth-order polynomial function as expected from ISO recommendations.

2.5. Overall uncertainties and compliance with dosimetry standards

The technical procedures adopted for measuring the dosimetric parameters were bound to comply with internationally acceptable recommendations for diode-based dosimeters in medical dosimetry (IEC 61674, 2012) due to the lack of similar standard protocols for radiation processing. Exceptions are those specifically addressed to alanine (ISO/ASTM 51607, 2013), radiochromic film (ISO/ASTM 51275, 2013), and routine dosimetry systems for use in radiation processing (ISO/-ASTM 51702, 2013).

The combined uncertainty of each performance characteristic was assessed by adding all the components (types A and B) of the standard uncertainties in quadrature (ISO/ASTM 51707, 2015). The corresponding expanded uncertainty was calculated with a coverage factor k = 2, providing a confidence level of about 95%.

The uncertainty budget of the data on the dose rate and dose is shown in Table 1.

Table 1
- Uncertainty budget of the dose rate and dose data.

Uncertainty Components	Standard Deviation	Type
Dose rate		
Current readings	0.1%	A
Electrometer accuracy	0.1%	B
Reference dose rate (IDAS-IAEA)	0.85%	B
Fit Current x Dose rate curve	0.7%	A
Temperature variation	0.35%	B
Combined uncertainty	***1.2%***	
Expanded uncertainty	***2.4%***	
Dose		
Dose rate uncertainty	1.2%	A/B
Irradiation time	0.4%	B
Fit Charge x Dose curve	0.2%	A
Combined uncertainty	***1.3%***	
Expanded uncertainty	***2.6%***	

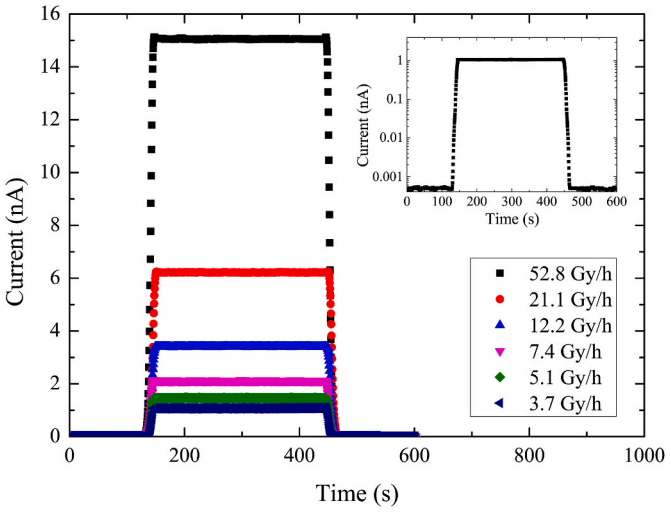

Fig. 1. - Induced current signals delivered by the same diode exposed to dose rates varying from 3.7 to 52.8 Gy/h. The inset plot shows an expanded view of the current signal recorded at 3.7 Gy/h with the background current measured before and after the irradiation.

3. Results and discussion

3.1. Dose rate response

The current signals delivered by the diode under exposure to different dose rates are presented in Fig. 1. As it can be seen, all of them feature rectangular profiles characterized by the flat region corresponding to the maximum induced current delivered by the diode when the radioactive source is at the irradiation position. The rise and the decay of the current signals are due to the up/down transit of the source, which agrees with the switching on/off time of the ^{60}Co facility system. The background current (≈1 pA), measured when the source is at the storage position, is almost constant regardless of the irradiation level. As shown in the inset plot of Fig. 1, even for the smallest dose rate, the background current is less than 0.1% of the induced current, which complies with this performance requirement (<0.1%) of the IEC 61674 standard. Furthermore, as the current to noise ratio is higher than 10^3, the effect of the background current on the current signals can be neglected, as shown again by the inset plot in Fig. 1.

The linear dependence of the induced current on the dose rate is shown in Fig. 2, where each induced current value corresponds to the average of 600 readings carried out with the source at the irradiation position. The current sensitivity (0.287 nA h/Gy), given by the slope of the dose rate response plot, confirms our earlier findings achieved with this diode under similar experimental conditions (Gonçalves et al., 2020).

For comparison, dose rate response calculations are performed using an expression for the current generated in a thin p-n junction irradiated by gamma rays (Osvay and Tárczy, 1975). The theoretical approach and assumptions made to allow this expression to be used in a PIN structure can be found in our previous article (Gonçalves et al., 2020). The excellent agreement between experimental and calculated dose rate

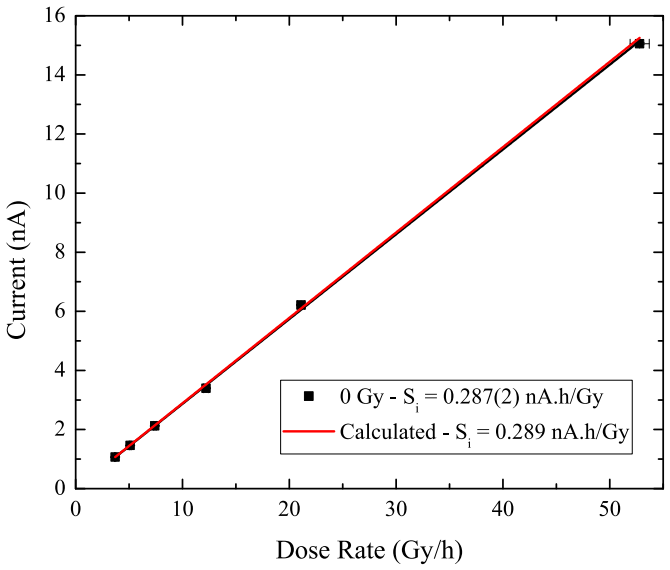

Fig. 2. - Experimental and calculated dose rate responses of a pristine diode covering the range of 3.7–52.8 Gy/h. The continuous line represents a linear fit to the measured values, whereas the dashed line shows the calculated results discussed in the text.

response, and their corresponding current sensitivities, is clearly evidenced in Fig. 2.

3.1.1. Repeatability

The repeatability of five consecutive current signals recorded at 3.7 Gy/h and 52.8 Gy/h dose rates are depicted in Fig. 3. All current signals are highly repetitive, yielding a maximum CV of only 0.2%, even for the lowest dose rate. This result is similar to or better than those found with dosimetry systems based on several diodes for clinical photon beams: Kumar et al. (2014) (0.5% for 6 MV–18 MV and ^{60}Co); Santos et al. (2014) (<1.0% for 6 MV). Furthermore, the repeatability results of the SFH206K adhere to AAPM 87-TG 62, 2005 and IEC 61674, 2012 protocols, which recommend a repeatability error of less than 1% for a diode used as a dosimeter.

3.1.2. Reproducibility

The residues of the current measurements carried out monthly over one semester at a dose rate of 52.8 Gy/h, with respect to the corresponding average value, 16.0 nA, are shown in Fig. 4. Each data point is the average of three current signals. The high reproducibility of the current data, better than 1%, complies with the reproducibility requirement (<2.0%) of the IEC 61674 standard.

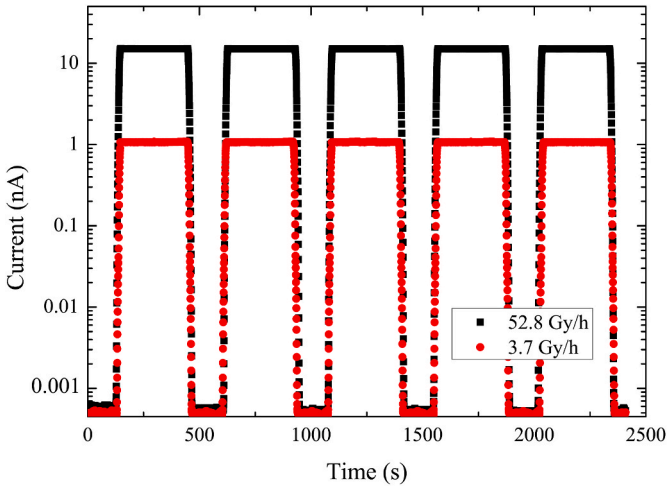

Fig. 3. - Five consecutive current signals recorded at 3.7 and 52.8 Gy/h dose rates. The repeatability parameter is better than 0.2%, even for the lowest dose rate.

3.1.3. Angular response

The directional response of the diode for incidence angles ranging from 0° to 90° is depicted in Fig. 5. All the current data were normalized to the current reading at 0°, i.e., when the radiation hits the front surface of the diode perpendicularly. As a result, the highest variation (27% at 90°) is much less than that assessed with infrared radiation at the maximum sensitivity wavelength (850 nm) disclosed by the diode manufacturer (inset plot in Fig. 5). The difference between the directional responses can be ascribed to their dependence on the incident radiation energy and, as expected, the lower energy, the more prominent is the angular response. It is important to note that the variation (1%) of the diode response due to a change of ±5° from the normal direction of incidence fully adheres to the recommendation (<3%) of the IEC 61674 standard.

3.2. Dose response

The dose responses of a pristine diode and after accumulating doses up to 15 kGy, fractioned in three steps of 5 kGy, are shown in Fig. 6. In the same figure, the calculated dose response, i.e., the charge assessed by integrating the expression for the current generated in a thin p-n junction irradiated by gamma rays (Osvay and Tárczy, 1975), as a function of the dose is also presented. For doses covering 200 Gy at 52.8 Gy/h, the linearity between charge and dose is evidenced in all data sets despite a slight dependence of the diode sensitivity on accumulated doses. The charge sensitivity of the diode irradiated to different doses decreases, as shown by the numerical values given in Table 2. Although the sensitivity variation is small, it must be less than 5% to comply with the stability performance requirements of the ISO/ASTM 51702 (2013) and ISO/-ASTM 52628 (2020) standard protocols for routine dosimeters in radiation processing. In this work, this condition is satisfied up to 15 kGy, which is the maximum accumulated dose that the diode can withstand before it becomes necessary to discard or re-calibrate it. The predicted reusability of the diode, almost 150 times for accumulated doses of 100 Gy per each use, depends on their dose history, but their low cost (US

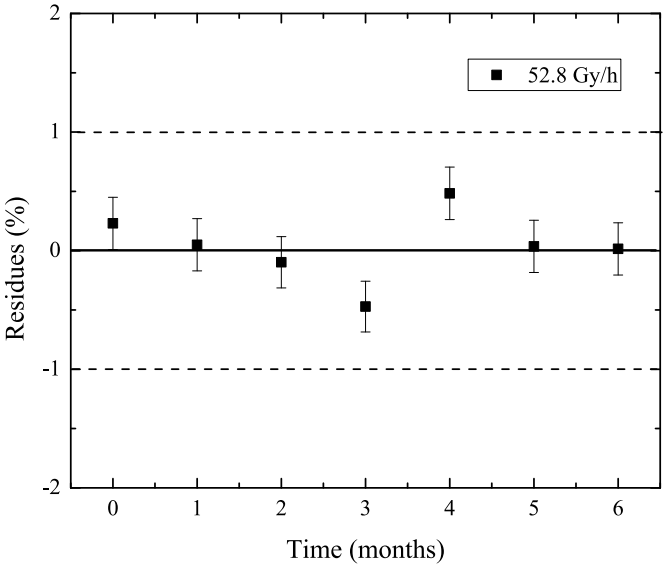

Fig. 4. - Residues of the current data from the average value of the measurements gathered at 52.8 Gy/h. The error bars represent the propagation of the uncertainties of each current reading. The zero of the vertical scale corresponds to the average value of all the measured currents, 16.0 nA.

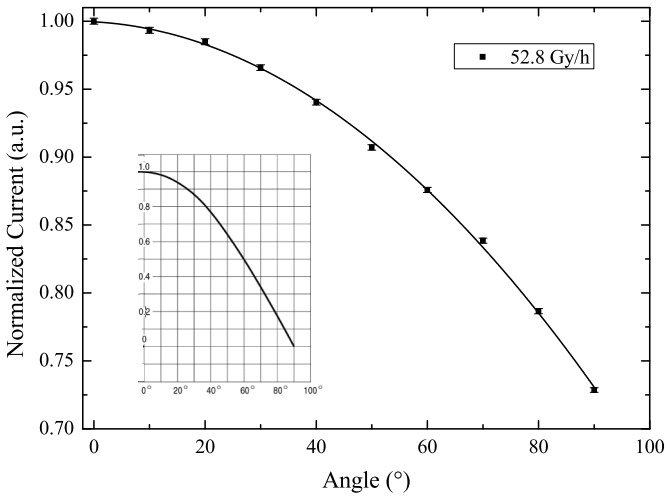

Fig. 5. - Directional response of the diode over the incidence angle range of 0 °–90°, obtained with gamma rays from ^{60}Co. The inset plot shows the angular response assessed with infrared radiation at the diode maximum sensitivity wavelength (850 nm) disclosed by the manufacturer.

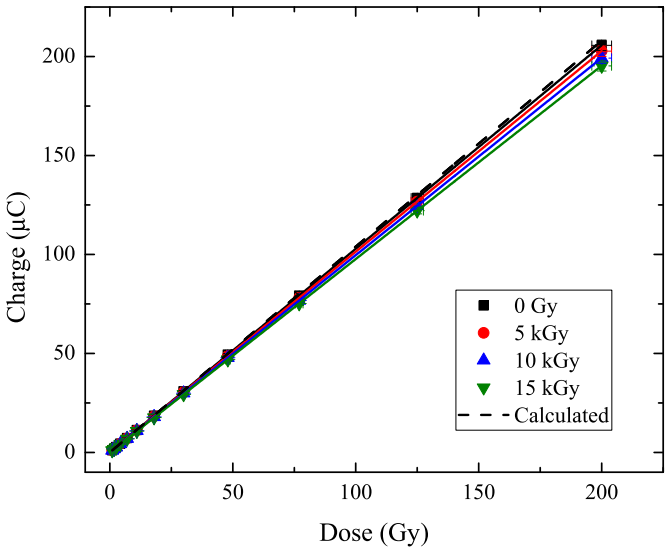

Fig. 6. - Dose response curves of a pristine diode (0 Gy) and irradiated to 5, 10, and 15 kGy. The dose range covered extends up to 200 Gy at 52.8 Gy/h. For comparison, the calculated dose response for the pristine diode is shown.

Table 2
Charge Sensitivity (S_q) of a pristine diode and irradiated up to 5, 10, and 15 kGy. The expanded uncertainty of the sensitivity is from the budget shown in Table 1.

Accumulated Dose (kGy)	S_q (μC/Gy)
0	1.029 ± 0.026
5	1.014 ± 0.026
10	0.997 ± 0.026
15	0.977 ± 0.025
Calculated	1.040

$1.00 each) renders them viable even as single-use dosimeters.

The dose-response dependence on the dose rate was investigated by irradiating the diode to 7 Gy at different dose rates (3.7–52.8 Gy/h). The residues of each charge reading from the average value of the whole data set are shown in Fig. 7. These results show that the dose rate effect is smaller than 2.5% and, therefore, within the limits of variation (<3%) of this performance characteristic established by the AAPM 87-TG 62 protocol.

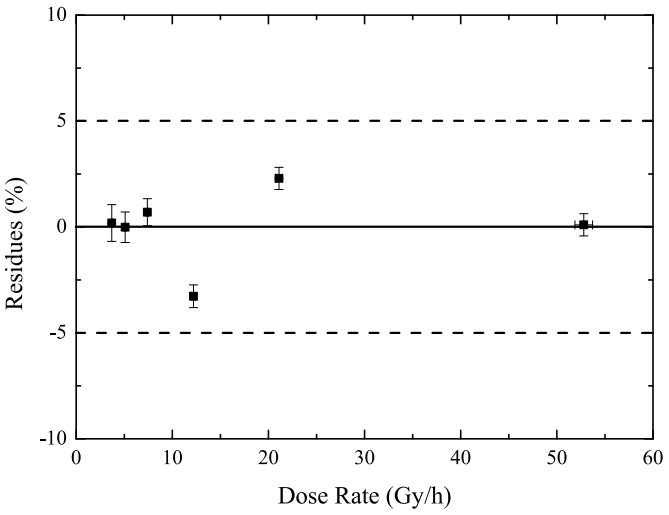

Fig. 7. - Dose response dependence on the dose rate between 3.7 Gy/h and 52.8 Gy/h. Regardless of the dose rate, the same diode was irradiated to 7 Gy.

3.3. Diode response as a routine dosimeter

Fig. 8 displays the diode and GAFChromic HD-V2 film readings against those assessed with the reference standard alanine. For both types of dosimeters, the data over the dynamic dose range are linearly fitted with similar angular coefficients of 0.9992 (diode) and 1.0015 (film). Therefore, the consistency between these two data sets can be quantified from their residues concerning the alanine dosimeters, as presented in Fig. 9. The trend of the data points reveals great agreement between the diode and alanine readings in the whole dose range. Concerning the GAFChromic HD-V2 film, its performance is very good except for doses below 100 Gy since they are close to the lowest limit of its operational range (10 Gy-1 kGy). However, variations in its response of less than 3%, besides being assigned by the manufacturer, also meet the recommendations (<5%) of ISO/ASTM 52628 (2020) for radiochromic films routinely applied in radiation processing.

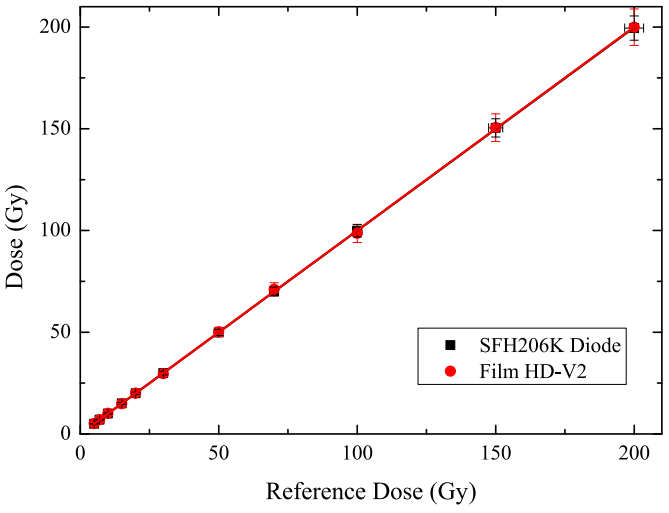

Fig. 8. - Dose response of the diode and radiochromic film against the alanine reference up to 200 Gy.

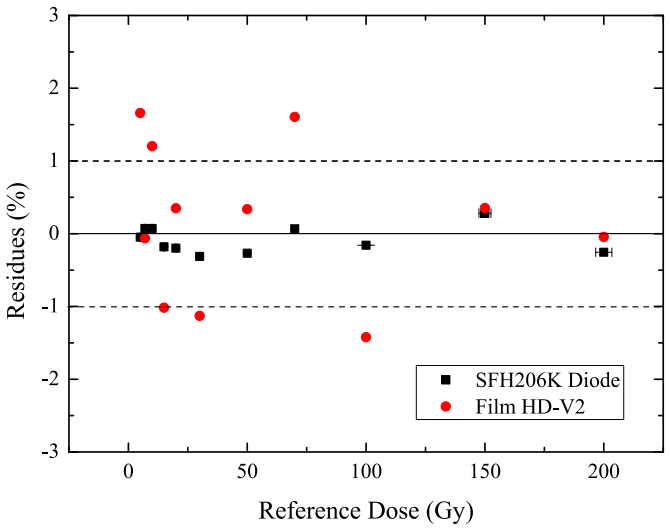

Fig. 9. - Residues of the diode and GAFChromic HD-V2 film readings from the corresponding alanine reference doses.

4. Conclusions

A dosimetry system based on a commercial PIN photodiode has been characterized in a ^{60}Co industrial facility under the same conditions of use in low-dose radiation processing applications. The limits of the performance characteristics, such as repeatability (0.2%), reproducibility (<1%), and angular dependence (<1% at 5°), comply with the requirements of standard protocols for radiation processing dosimetry. The stable response of the diode, in good agreement with that of chemical dosimeters, is largely due to the small current sensitivity decay (0.3%/kGy) with increasing accumulated dose. It improves both the stability and inherent precision of the dose rate measurements (2.3%). The results fully validate both the data published in our previous papers and ensure the reliable performance of the diode as a routine dosimeter for low-dose radiation processing.

Credit author statement

J. A. C. Gonçalves: Methodology, Formal analysis, Investigation, Resources, Data Curation, Funding acquisition, Review & Editing, A. Mangiarotti: Methodology, Formal analysis, Review & Editing, C. C. Bueno: Conceptualization, Methodology, Formal analysis, Writing - Original Draft, Writing - Review & Editing, Supervision.

Declaration of competing interest

The authors declare that they have no known competing financial interests or personal relationships that could have appeared to influence the work reported in this paper.

Acknowledgments

The authors highly acknowledge the collaboration of Eng. Elisabeth S. R. Somessari from the Gamma Irradiators staff (IPEN-CNEN/SP) for her indispensable help during the irradiations. The authors also thank the staff from the Packaging and System Integration Laboratory at Centro de Tecnologia da Informação Renato Archer (CTI-Renato Archer, Campinas/SP), for the electrical characterization of the diodes. This work is partially supported by IPEN-CNEN/SP (DPDE Edital 04/2017). AM acknowledges two fellowships by CNPq (contracts n° 306331/2016–0 and 311915/2020–5).

References

AAPM 87-TG 62, 2005. Diode in-vivo dosimetry for patients receiving external beam radiation therapy. In: Report of Task Group 62 (American Association of Physicists in Medicine) of the Radiation Therapy Committee. Med. Phys. Publishing.

Andjelković, M.S., Ristić, G.S., 2013. Feasibility study of a current mode gamma radiation dosimeter based on a commercial PIN photodiode and a custom-made auto-ranging electrometer. Nucl. Technol. Radiat. Protect. 28 (1), 73–83, 10.2298NTRP/1301073A.

Andjelković, M.S., Ristić, G.S., 2015. Current mode response of phototransistors to gamma radiation. Radiat. Meas. 75, 29–38. https://doi.org/10.1016/j.radmeas.2015.03.005.

Bailey, M., Sephton, J.P., Sharpe, P.H.G., 2009. Monte Carlo modeling and real-time dosemeter measurements of dose rate distribution at a ^{60}Co industrial irradiation plant. Radiat. Phys. Chem. 78 (3), 453–456. https://doi.org/10.1016/j.radphyschem.2009.03.024.

Barthe, J., 2001. Electronic dosimeters based on solid-state detectors. Nucl. Instrum. Methods B 184, 158–189. https://doi.org/10.1016/S0168-583X(01)00711-X.

Bruzzi, M., Bucciolini, M., Casati, M., Menichelli, D., Talamonti, C., Piemonte, C., Svensson, B.G., 2007. Epitaxial silicon devices for dosimetry applications. Appl. Phys. Lett. 90, 172109 https://doi.org/10.1063/1.2723075.

Bueno, C.C., Camargo, F., Gonçalves, J.A.C., Pascoalino, K., Mangiarotti, A., Tuominen, E., Härkönen, J., 2022. Performance characterization of dosimeters based on radiation-hard silicon diodes in gamma radiation processing. Front. Sensors 3, 770482. https://doi.org/10.3389/fsens.2022.770482.

Casati, M., Bruzzi, M., Bucciolini, M., Menichelli, D., Scaringella, M., Piemonte, C., Fretwurst, E., 2005. Characterization of standard and oxygenated float zone Si diodes under radiotherapy beams. Nucl. Instrum. Methods 552, 158–162. https://doi.org/10.1016/j.nima.2005.06.025.

Dixon, R.L., Ekstrand, K.E., 1982. Silicon diode dosimetry. Int. J. Appl. Radiat. Isot. 33, 1171–1176.

EL-Degwi, M.S., Gabarty, A., 2015. Morphological changes induced by thermal treatment and gamma irradiation on the males' hind legs of *Spodoptera littoralis* (Noctuidae; Lepidoptera). J. Radiat. Res. Appl. Sci. 8, 508–515. https://doi.org/10.1016/.jrras.2015.06.002.

Fuochi, P.G., Lavalle, M., Corda, U., Recupero, S., Bosetto, A., Baschieri, V., Kovács, A., 2004. In-plant calibration and use of power transistors for process controlo f gamma and eléctron beam facilities. Radiat. Phys. Chem. 71, 383–386. https://doi.org/10.1016/j.radphyschem.2004.03.034.

Gilar, O., Petr, I., 1985. Silicon photodiode as a detector of exposure rate. Nucl. Instrum. Methods 234, 566–572. https://doi.org/10.1016/0168-9002(85)91009-5.

Gonçalves, J.A.C., Mangiarotti, A., Bueno, C.C., 2020. Current response stability of a commercial PIN photodiode for low dose radiation processing applications. Radiat. Phys. Chem. 167, 108276–108279. https://doi.org/10.1016/j.radphyschem.2019.04.026.

Gonçalves, J.A.C., Mangiarotti, A., Asfora, V.K., Khoury, H.J., Bueno, C.C., 2021. The response of low-cost photodiodes for dosimetry in electron beam processing. Radiat. Phys. Chem. 181, 109335–109342. https://doi.org/10.1016/j.radphyschem.2020.109335.

Grusell, E., Rikner, G., 1984. Radiation damage induced dose rate non-linearity in an n-type silicon detector. Acta Radiol. Oncol. 23 (6), 465–469. https://doi.org/10.3109/02841868409136050.

ICRU Report 80, 2008. International Commission on Radiation Units and Measurements, Dosimetry Systems for Use in Radiation Processing, ICRU Report 80 (International Commission on Radiation Units and Measurements, 2008. https://doi.org/10.1093/jicru/ndn031.

IEC 61674, 2012. International Electrotechnical Commission, Medical Electrical Equipment - Dosimeters with Ionization Chambers and/or Semiconductor Detectors as Used in X-Ray Diagnostic Imaging, second ed.

ISO/ASTM 51275, 2013. Practice for Use of a Radiochromic Film Dosimetry System. https://doi.org/10.1520/ISOASTM51275-13.

ISO/ASTM 51607, 2013. Practice for Use of the Alanine-EPR Dosimetry System. https://doi.org/10.1520/ISOASTM51607-13.

ISO/ASTM 51649, 2015. Practice for Dosimetry in an Electron Beam Facility for Radiation Processing at Energies between 300 keV and 25 MeV, third ed. https://doi.org/10.1520/ISOASTM51649-15.

ISO/ASTM 51702, 2013. Standard Practice for Dosimetry in a Gamma Facility for Radiation Processing, third ed.

ISO/ASTM 51707, 2015. Standard Guide for Estimation of Measurement Uncertainty in Dosimetry for Radiation Processing, third ed. https://doi.org/10.1520/ISOASTM51707-15 2015.

ISO/ASTM 51939, 2017. Standard Practice for Blood Irradiation Dosimetry, fourth ed.

ISO/ASTM 52628, 2020. Standard Practice for Dosimetry in Radiation Processing, second ed.

Kumar, R., Sharma, S.D., Philomina, A., Topkar, A., 2014. Dosimetric Characteristics of a PIN Diode for Radiotherapy Application Technology in Cancer Research and Treatment, 13, pp. 360–367. https://doi.org/10.7785/tcrt.2012.500388, 4.

Majer, M., Roguljić, M., Knežević, Z., Starodumov, A., Ferenček, D., Brigljević, V., Mihaljević, B., 2019. Dose mapping of the panoramic ^{60}Co gamma irradiation facility - GEANT4 simulation and measurements. Appl. Radiat. Isot. 154, 108824 https://doi.org/10.1016/j.apradiso.2019.108824.

Möhlmann, J.H.F., 1981. The use of solar cells for continuous recording of absorbed dose in the product during radiation sterilization. In: Biomedical Dosimetry, Proceedings of Symposium, Vienna, 1981. IAEA Publication STI/PUB/567, p. 563.

Moll, M., 2018. Displacement damage in silicon detectors for high energy physics. IEEE Trans. Nucl. Sci. 65 (8), 1561–1582. https://doi.org/10.1109/TNS.2018.2819506.

Muller, A.C., 1970a. The "n" on "p" solar-cell dose-rate meter. In: Holm, N.W., Berry, R.J. (Eds.), Manual on Radiation Dosimetry, p. 423. New York.

Muller, A.C., 1970b. The "p" on "n" solar-cell integrating dosimeter. In: Holm, N.W., Berry, R.J. (Eds.), Manual on Radiation Dosimetry, p. 429. New York.

Oliveira, C., Salgado, J., Carvalho, A.F., 2000. Dose rate determinations in the Portuguese Gamma Irradiation Facility: Monte Carlo simulations and measurements. Radiat. Phys. Chem. 58 (3), 279–285. https://doi.org/10.1016/S0969-806X(99)00462-4.

Osvay, M., Stenger, V., Földiak, G., 1975. Silicon detectors for measurement of high exposure rate gamma rays. In: Biomedical Dosimetry, Proceedings of Symposium, Vienna, 1974. IAEA Publication STI/PUB/401, p. 623.

Osvay, M., Tárczy, K., 1975. Measurement of γ-dose rates by n- and p-type semiconductor detectors. Phys. Status Solidi 27, 285–290.

Rikner, G., Grusell, E., 1987. General specifications for silicon semiconductors for use in radiation dosimetry. Phys. Med. Biol. 32 (9), 1109–1117. https://doi.org/10.1088/0031-9155/32/9/004.

Salem, H.M., Fouda, M.A., Abas, A.A., Ali, W.M., Gabarty, A., 2014. Effects of gamma irradiation on the development and reproduction of the greasy cutworm, *Agrotis ipsilon* (Hufn.). J. Radiat. Res. Appl. Sci. 7, 110–115. https://doi.org/10.1016/.jrras.2013.12.007.

Santos, T.C., Neves-Junior, W.F.P., Gonçalves, J.A.C., Haddad, C.M.K., Harkonen, J., Bueno, C.C., 2014. Characterization of miniature rad-hard silicon diodes as dosimeters for small fields of photon beams used in radiotherapy. Radiat. Meas. 71, 396–401. https://doi.org/10.1016/j.radmeas.2014.08.002.

Sephton, J.P., et al., 2007. Dose mapping of a 60Co industrial irradiation plant using an electronic data recording system, static measurements, and mathematical modeling. Radiat. Phys. Chem. 76 (11), 1820–1825. https://doi.org/10.1016/j.radphyschem.2007.02.110.

Shastry, S., Ramya, B., Ninan, J., Srinidhi, G.C., Bhat, S.S., Fernandes, D.J., 2013. Linear accelerator: a reproducible, efficacious, and cost-effective alternative for blood irradiation. Transfus. Apher. Sci. 49, 528–532. https://doi.org/10.1016/j.transci.2013.03.007.